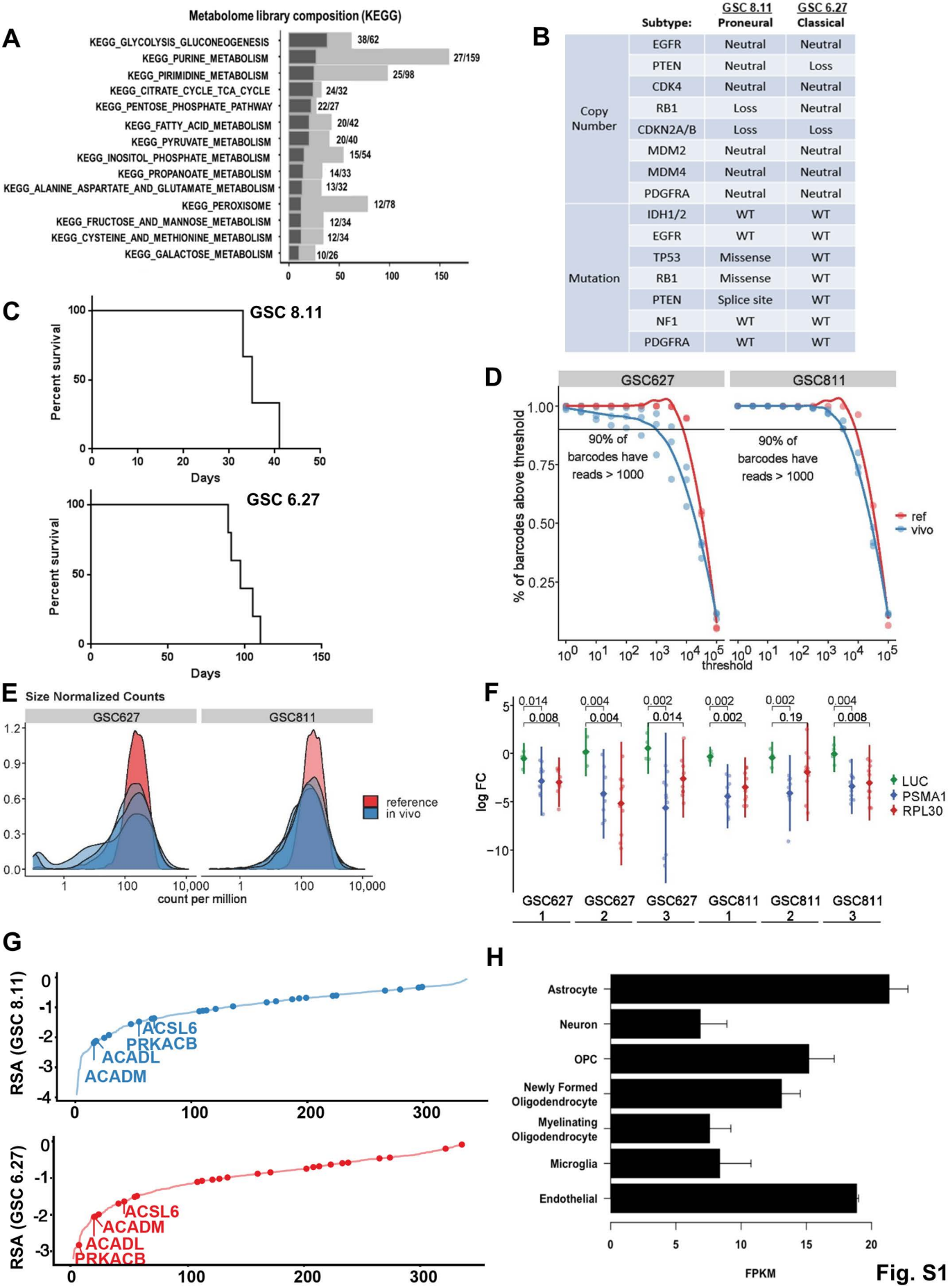
A
Metabolome library composition (KEGG)
KEGG_GLYCOLYSIS_GLUCONEOGENESIS 38/62
KEGG_PURINE_METABOLISM 27/159
KEGG_PIRIMIDINE_METABOLISM 25/98
KEGG_CITRATE_CYCLE_TCA_CYCLE 24/32
KEGG_PENTOSE_PHOSPHATE_PATHWAY 22/27
KEGG_FATTY_ACID_METABOLISM 20/42
KEGG_PYRUVATE_METABOLISM 20/40
KEGG_INOSITOL_PHOSPHATE_METABOLISM 15/54
KEGG_PROPANOATE_METABOLISM 14/33
KEGG_ALANINE_ASPARTATE_AND_GLUTAMATE_METABOLISM 13/32
KEGG_PEROXISOME 12/78
KEGG_FRUCTOSE_AND_MANNOSE_METABOLISM 12/34
KEGG_CYSTEINE_AND_METHIONINE_METABOLISM 12/34
KEGG_GALACTOSE_METABOLISM 10/26
0 50 100 150
B
Subtype: GSC 8.11 Proneural GSC 6.27 Classical
Copy Number
EGFR Neutral Neutral
PTEN Neutral Loss
CDK4 Neutral Neutral
RB1 Loss Neutral
CDKN2A/B Loss Loss
MDM2 Neutral Neutral
MDM4 Neutral Neutral
PDGFRA Neutral Neutral
Mutation
IDH1/2 WT WT
EGFR WT WT
TP53 Missense WT
RB1 Missense WT
PTEN Splice site WT
NF1 WT WT
PDGFRA WT WT
C
GSC 8.11
Percent survival
Days
GSC 6.27
Percent survival
Days
D
GSC627
GSC811
% of barcodes above threshold
90% of barcodes have reads > 1000
threshold
ref
vivo
E
Size Normalized Counts
GSC627
GSC811
reference
in vivo
count per million
F
log FC
0.014 0.008
0.004 0.004
0.002 0.014
0.002 0.002
0.002 0.19
0.004 0.008
LUC
PSMA1
RPL30
GSC627 1
GSC627 2
GSC627 3
GSC811 1
GSC811 2
GSC811 3
G
RSA (GSC 8.11)
ACSL6
PRKACB
ACADL
ACADM
RSA (GSC 6.27)
ACSL6
ACADM
ACADL
PRKACB
H
Astrocyte
Neuron
OPC
Newly Formed Oligodendrocyte
Myelinating Oligodendrocyte
Microglia
Endothelial
FPKM

Fig. S1

Figure S1: **Details of metabolome screen in human GSCs. a.** KEGG pathway composition of the metabolome shRNA library. Dark gray bars represent the genes covered by the screen within the total genes that constitute the pathway (light gray). **b.** List of genomic events and driver mutations that characterized the GBM models used for the screen (GSC 8.11 and 6.27). **c.** Kaplan-Meier survival analysis of animals with intracranial tumors generated from injecting 1 x 10^6 GSC 8.11 or 6.27 cells. **d.** Percentage of shRNA-associated barcodes recovered above each indicated threshold of read counts for transduced GSCs (ref) and tumors (*in vivo*). Fold change (log2) distributions of positive (PMSA1, proteasome subunit alpha type-1, and RPL30, ribosomal protein L30) and negative (Luciferase) control shRNAs. **e.** Density distribution of shRNA-associated barcodes (size normalized counts) for transduced GSCs (references) and three tumor replicates (*in vivo*) infected with the metabolome shRNA lentiviral library. **f.** Fold change (log2) distributions of positive (PMSA1, proteasome subunit alpha type-1, and RPL30, ribosomal protein L30) and negative (Luciferase) control shRNAs. **g.** Gene-rank analysis highlighting the behavior of genes involved in fatty acid metabolism (*ACADM*, *ACADL*, *PRKACB* and *ACSL6*) in *in vivo* screens executed in two independent GSC models: GSC 8.11 and GSC 6.27 (RSA = redundant shRNA activity, logP). **h.** Relative abundance of *ACADM* in brain cells expressed as Fragments Per Kilobase Of Exon Per Million Fragments Mapped (FPKM, data from RNAseq database from Ben Barres lab at Stanford (available at https://web.stanford.edu)

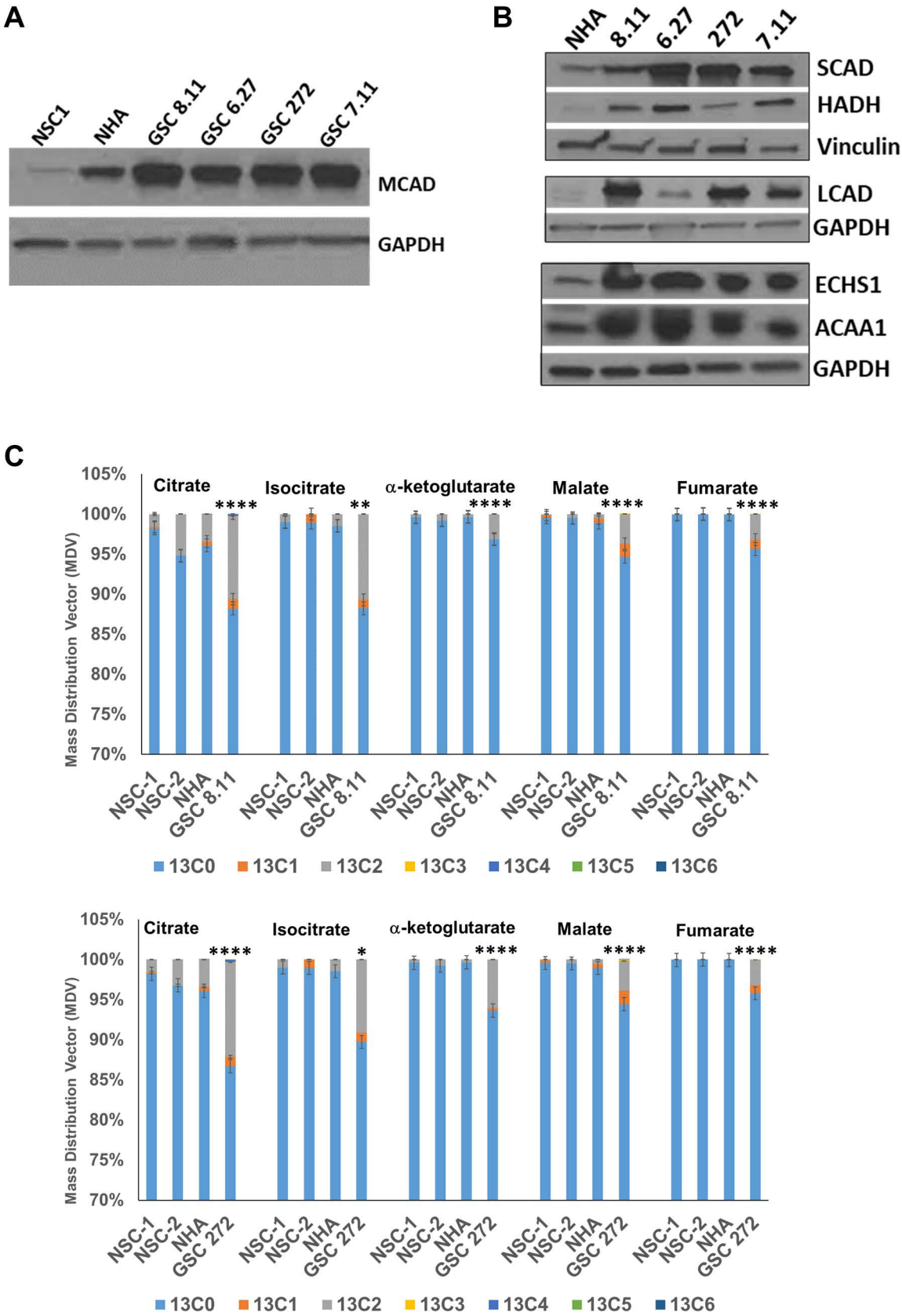
A
NSC1
NHA
GSC 8.11
GSC 6.27
GSC 272
GSC 7.11
MCAD
GAPDH
B
NHA
8.11
6.27
272
7.11
SCAD
HADH
Vinculin
LCAD
GAPDH
ECHS1
ACAA1
GAPDH
C
Mass Distribution Vector (MDV)
105%
100%
95%
90%
85%
80%
75%
70%
Citrate
Isocitrate
α-ketoglutarate
Malate
Fumarate
****
**
****
****
****
NSC-1
NSC-2
NHA
GSC 8.11
13C0
13C1
13C2
13C3
13C4
13C5
13C6
Mass Distribution Vector (MDV)
Citrate
Isocitrate
α-ketoglutarate
Malate
Fumarate
****
*
****
****
****
NSC-1
NSC-2
NHA
GSC 272
13C0
13C1
13C2
13C3
13C4
13C5
13C6

Fig. S2

Figure S2: Fatty acid oxidation fuels oxidative metabolism in GBM cells. a. Representative immunoblot of MCAD expression in NHAs and NSCs in comparison with different GSCs models. GAPDH served as loading control. **b.** Representative immunoblot of FAO enzymes expression in NHAs compared to GSCs models. Vinculin and GAPDH served as loading controls. **c.** Isotopologue patterns for incorporation of ^{13}C- labeled oleate into TCA cycle intermediates, as measured by LC-MS in NHAs and GSCs in basal conditions in GSCs 8.11 and 272. Cells were cultured with ^{13}C oleate for 6 hours prior to sample collection. n = 4 biological replicates, error = +/- SD. **P*= 0.0129, ***P*= 0.0014, *****P* <0.0001.

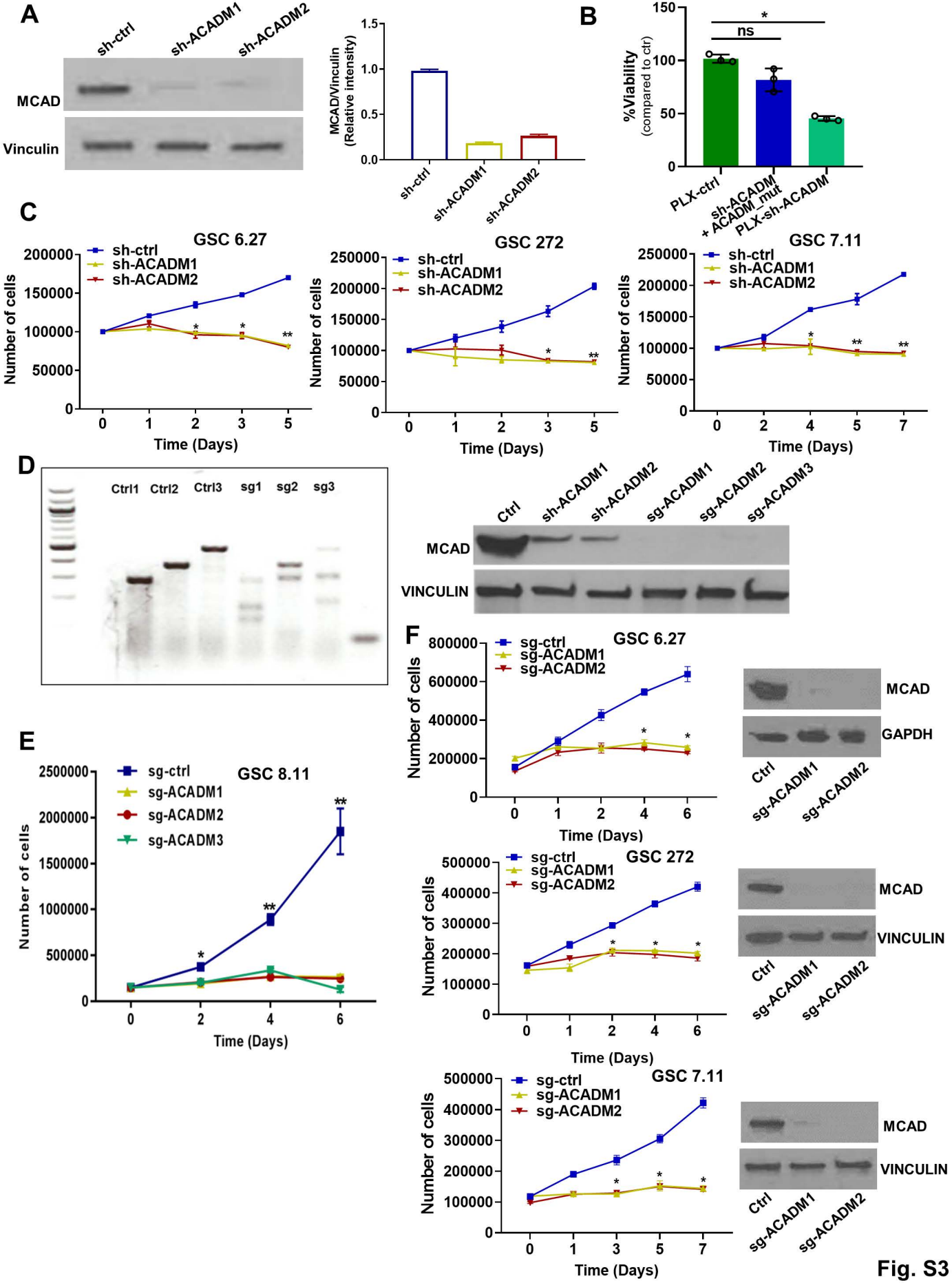
A
sh-ctrl
sh-ACADM1
sh-ACADM2
MCAD
Vinculin
MCAD/Vinculin (Relative intensity)
B
%Viability (compared to ctr)
ns
*
PLX-ctrl
sh-ACADM + ACADM_mut
PLX-sh-ACADM
C
GSC 6.27
GSC 272
GSC 7.11
sh-ctrl
sh-ACADM1
sh-ACADM2
Number of cells
Time (Days)
D
Ctrl1
Ctrl2
Ctrl3
sg1
sg2
sg3
Ctrl
sh-ACADM1
sh-ACADM2
sg-ACADM1
sg-ACADM2
sg-ACADM3
MCAD
VINCULIN
E
GSC 8.11
sg-ctrl
sg-ACADM1
sg-ACADM2
sg-ACADM3
Number of cells
Time (Days)
F
GSC 6.27
GSC 272
GSC 7.11
sg-ctrl
sg-ACADM1
sg-ACADM2
Number of cells
Time (Days)
MCAD
GAPDH
VINCULIN
Ctrl
sg-ACADM1
sg-ACADM2

Fig. S3

Figure S3: MCAD ablation dramatically affects GSC growth *in vitro*. a. Representative immunoblot (left) and quantification (right) of MCAD expression in GSC 8.11 infected with *ACADM*-targeting or control shRNA. Vinculin served as a loading control. **b.** GSC 8.11 cells were stably transfected with mutant *ACADM*- expressing vector or with an empty vector (PLX). The number of viable cells (as percentage of the ctrl) was assessed by Trypan Blue exclusion after genetic silencing. Values are expressed as mean ± SD of three independent experiments; *P* values were generated using Kruskal–Wallis ANOVA. Dunn's test for comparison among groups **P* <0.05. **c.** Growth curve of GSCs 6.27, 272, and 7.11 upon shRNA-mediated *ACADM* knockdown. Values represent the mean ± SD of three independent experiments; *P* values were generated using Kruskal–Wallis ANOVA. Dunn's test for comparison among groups GSCs 6.27 **P*< 0.04; ***P* = 0.0051. GSCs 272, * *P* = 0.0132, ** *P* = 0.0078. GSCs 7.11, * *P* = 0.034; ** *P* ≤ 0.004. **d.** (Left) Analysis of Cas9 activity by T7 endonuclease I assay. GSCs were transfected and total genomic DNA was isolated 72 h post transfection for subsequent T7EI cleavage. (Right) MCAD knockdown/knockout efficiency of shRNAs/sgRNAs determined by immunoblot. Vinculin served as loading control. **e.** Growth curve of GSC 8.11 cells carrying three independent sgRNA-mediated *ACADM* deletions, compared to a sgRNA control. Day 0 was defined as starting 48 hours post-puromycin selection. Values represent the mean ± SD of three independent experiments. *P* values were generated using Kruskal–Wallis ANOVA. Dunn's test for comparison among groups * *P* =0.0146, ** *P* ≤ 0.01. **f.** (Left) Growth curve of GSCs 6.27, 272, and 7.11 upon sgRNA-mediated *ACADM* knockout. Values represent the mean ± SD of three independent experiments; *P* values were generated using Kruskal–Wallis ANOVA. Dunn's test for comparison among groups GSCs 6.27 * *P* < 0.03; GSCs 272, * *P* ≤ 0.02. GSCs 7.11, * *P* ≤ 0.04. (Right) Representative immunoblot of MCAD expression in GSC 6.27, 272, 7.11 infected with *ACADM*-targeting or control sgRNA. Vinculin or GAPDH served as a loading control.

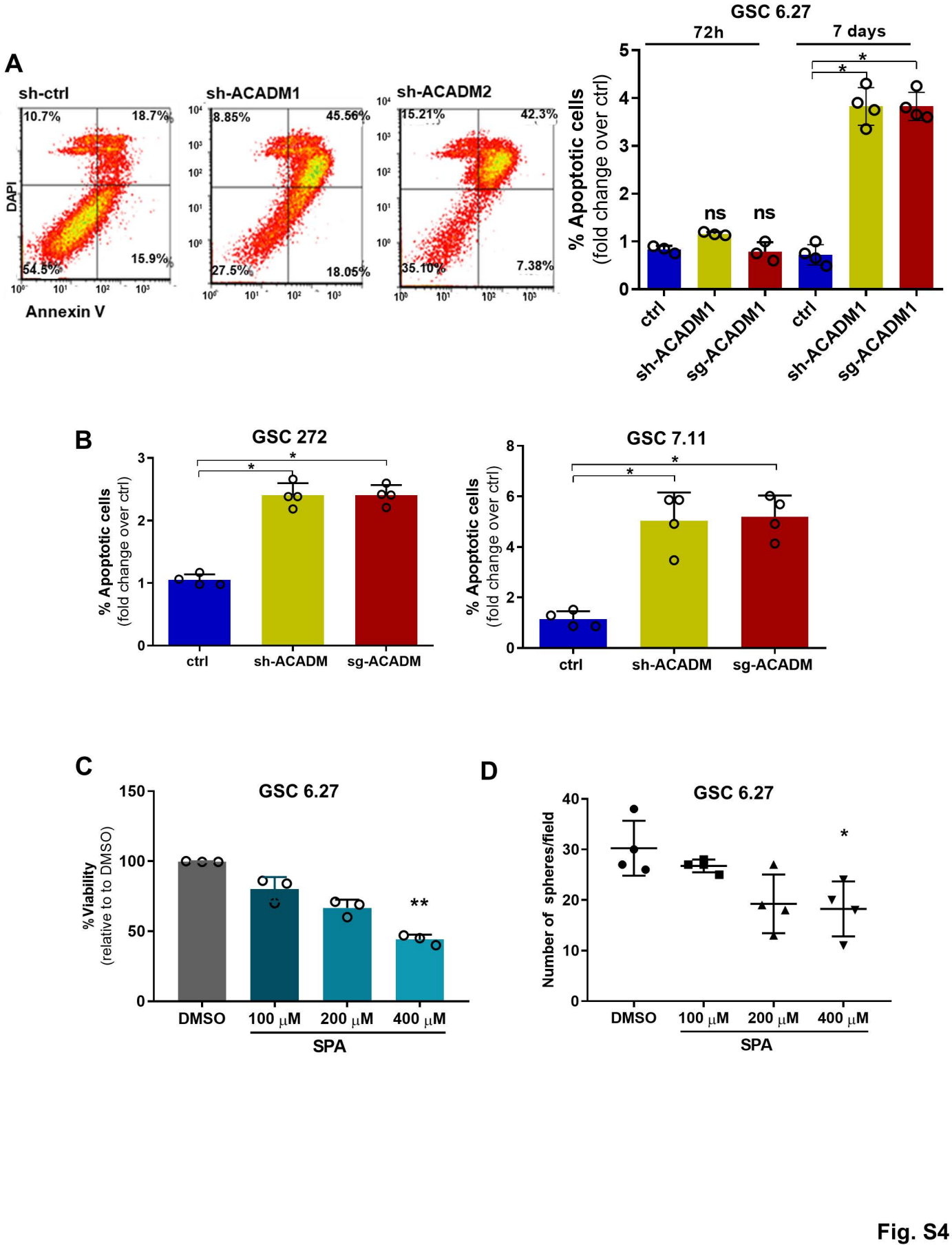
A
sh-ctrl
sh-ACADM1
sh-ACADM2
10.7%
18.7%
54.5%
15.9%
8.85%
45.56%
27.5%
18.05%
15.21%
42.3%
35.10%
7.38%
DAPI
Annexin V
GSC 6.27
72h
7 days
% Apoptotic cells
(fold change over ctrl)
ns
ns
ctrl
sh-ACADM1
sg-ACADM1
B
GSC 272
GSC 7.11
% Apoptotic cells
(fold change over ctrl)
ctrl
sh-ACADM
sg-ACADM
C
GSC 6.27
% Viability
(relative to to DMSO)
DMSO
100 μM
200 μM
400 μM
SPA
D
GSC 6.27
Number of spheres/field
DMSO
100 μM
200 μM
400 μM
SPA

Fig. S4

Figure S4: MCAD inhibition triggers apoptotic cell death and attenuates proliferative capacity and sphere-forming efficiency in GSCs *in vitro*. a. (Left) Representative scatter plot showing Annexin V and DAPI staining in GSC 8.11 cells upon MCAD knockdown (7 days post-puromycin selection) as measured by flow cytometry. (Right) Quantification of apoptosis in GSC 6.27 infected with anti-*ACADM* shRNA/shRNA by Annexin V. Staining was evaluated by flow cytometry at 72 hours and 7 days after puromycin selection. Values represent the mean ± SD of three or four independent experiments; *P* values were generated using Kruskal–Wallis ANOVA. Dunn's test for comparison among groups $*P < 0.05$. **b.** Quantification of apoptosis in GSC 272, 7.11 infected with anti-*ACADM* shRNA/sgRNA by Annexin V. Staining was evaluated by flow cytometry at day 7 after puromycin selection. Values represent the mean ± SD of four independent experiments; *P* values were generated using Kruskal–Wallis ANOVA. Dunn's test for comparison among groups 272 $*P < 0.03$, 7.11 $*P \leq 0.04$. **c.** Cell viability assessed by Trypan Blue exclusion of GSC 6.27 treated with indicated concentration of SPA. Mean values ± SD of three biologically independent replicates. *P* values were generated using Kruskal–Wallis ANOVA. Dunn's test for comparison among groups $**P = 0.006$ **d.** Dot plot showing GSCs 6.27 sphere formation efficiency (SFE) upon SPA treatment at different concentrations. DMSO was used as control. Values represent the mean ± SD of four independent experiments; *P* values were generated using Kruskal–Wallis ANOVA. Dunn's test for comparison among groups $*P = 0.0327$.

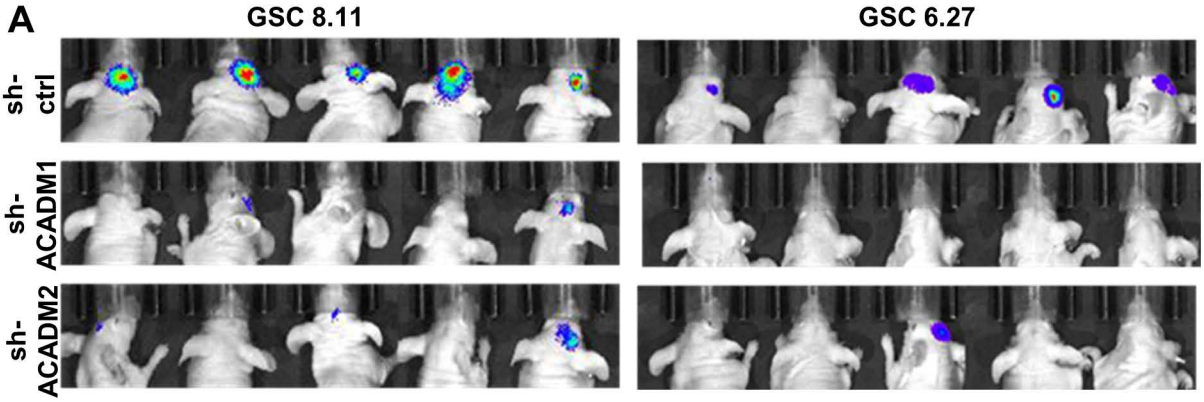
A
GSC 8.11
GSC 6.27
sh-ctrl
sh-ACADM1
sh-ACADM2

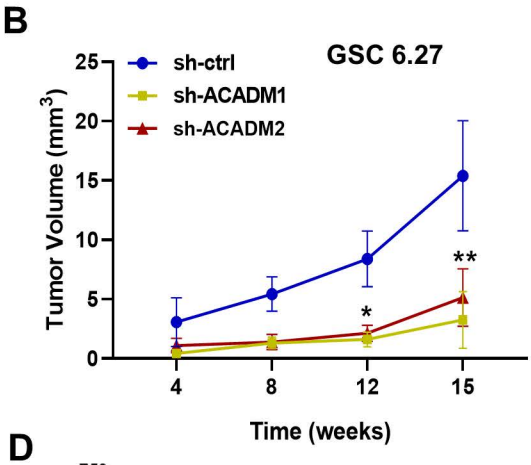
B
GSC 6.27
sh-ctrl
sh-ACADM1
sh-ACADM2
Tumor Volume (mm3)
Time (weeks)
*
**

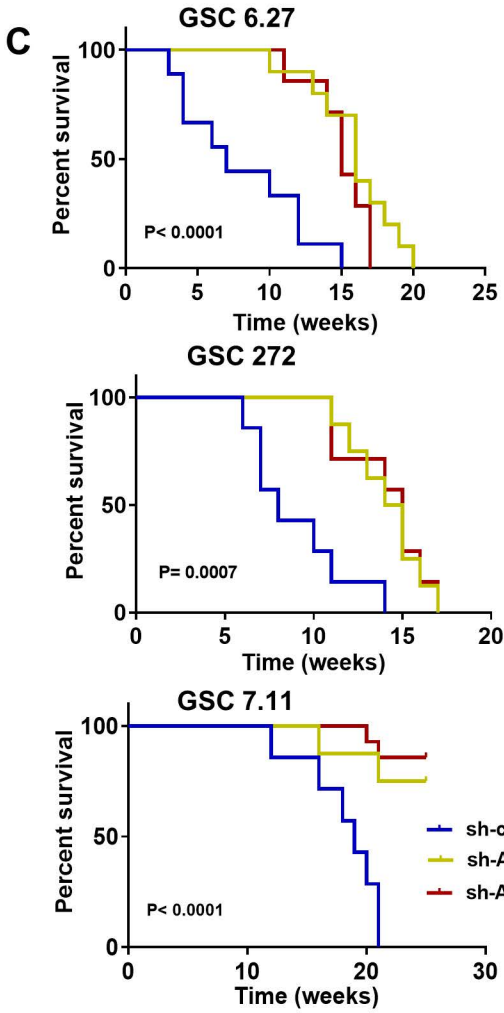
C
GSC 6.27
Percent survival
P< 0.0001
Time (weeks)
GSC 272
P= 0.0007
GSC 7.11
P< 0.0001
sh-ctrl
sh-ACADM1
sh-ACADM2

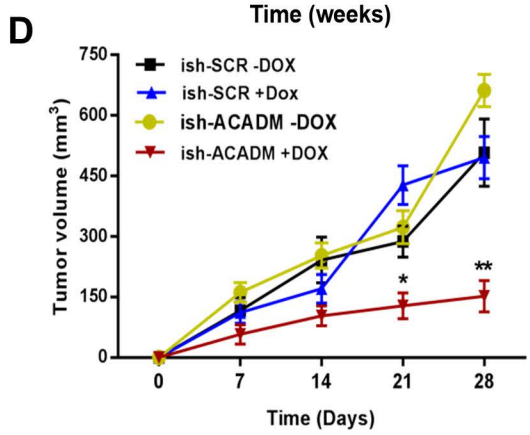
D
ish-SCR -DOX
ish-SCR +Dox
ish-ACADM -DOX
ish-ACADM +DOX
Tumor volume (mm3)
Time (Days)
*
**

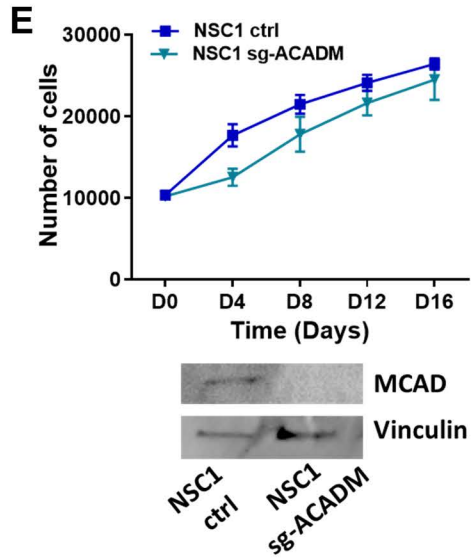
E
NSC1 ctrl
NSC1 sg-ACADM
Number of cells
Time (Days)
MCAD
Vinculin
NSC1 ctrl
NSC1 sg-ACADM

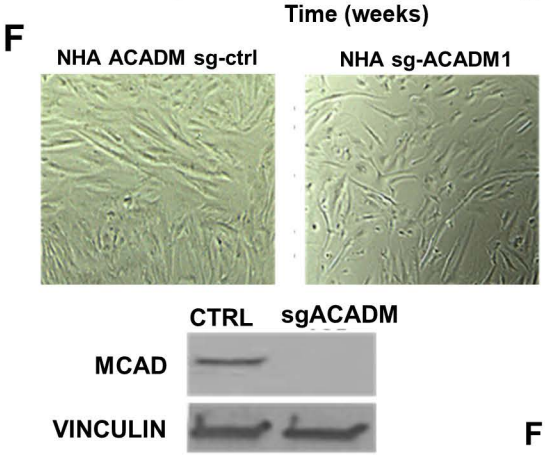
F
NHA ACADM sg-ctrl
NHA sg-ACADM1
CTRL
sgACADM
MCAD
VINCULIN

Fig. S5

Figure S5: MCAD ablation/inhibition impacts tumor formation of GSCs *in vivo*. a. Luciferase imaging of representative tumors 30 days (GSC 8.11) or 60 days (GSC 6.27) post-implantation. **b.** Quantification of tumor progression after implantation of GSCs 6.27 as measured by MR volumetry (n = 8 mice per group). Data represent mean ± SEM. *P* values were generated using Kruskal–Wallis ANOVA. Dunn's test for comparison among groups **P* =0.0121, ***P* = 0.0047. **c.** Kaplan-Meier survival analysis upon *in vivo* implantation of GSCs 6.27, 272 and 7.11. For sh-ctrl, sh-*ACADM1*, sh-*ACADM2*, n = 8 mice per group. *P* values were generated using log-rank test. ****P* = 0.0007, *****P* < 0.0001. **d.** Effect of shRNA-mediated knockdown on tumor growth in GSC 8.11 cells with induced (doxycycline) MCAD depletion 20 days after subcutaneous implantation. Day 0 indicates the beginning of doxycycline treatment (n = 5 mice per group). Values represent the mean ± SD of three independent experiments; *P* values were generated using Kruskal–Wallis ANOVA. Dunn's test for comparison among groups **P* = 0.036, ***P* = 0.003; **e.** (Top) Growth curve of NSCs infected with sgRNA targeting either *ACADM* or GFP. Values represent the mean ± SD of three independent experiments and (Bottom) representative immunoblot. Vinculin served as loading control. **f.** Representative images (top) of NHAs upon MCAD depletion at 7 days from the beginning of the growth curve shown in Figure 2H and corresponding immunoblot (bottom). Vinculin served as loading control.

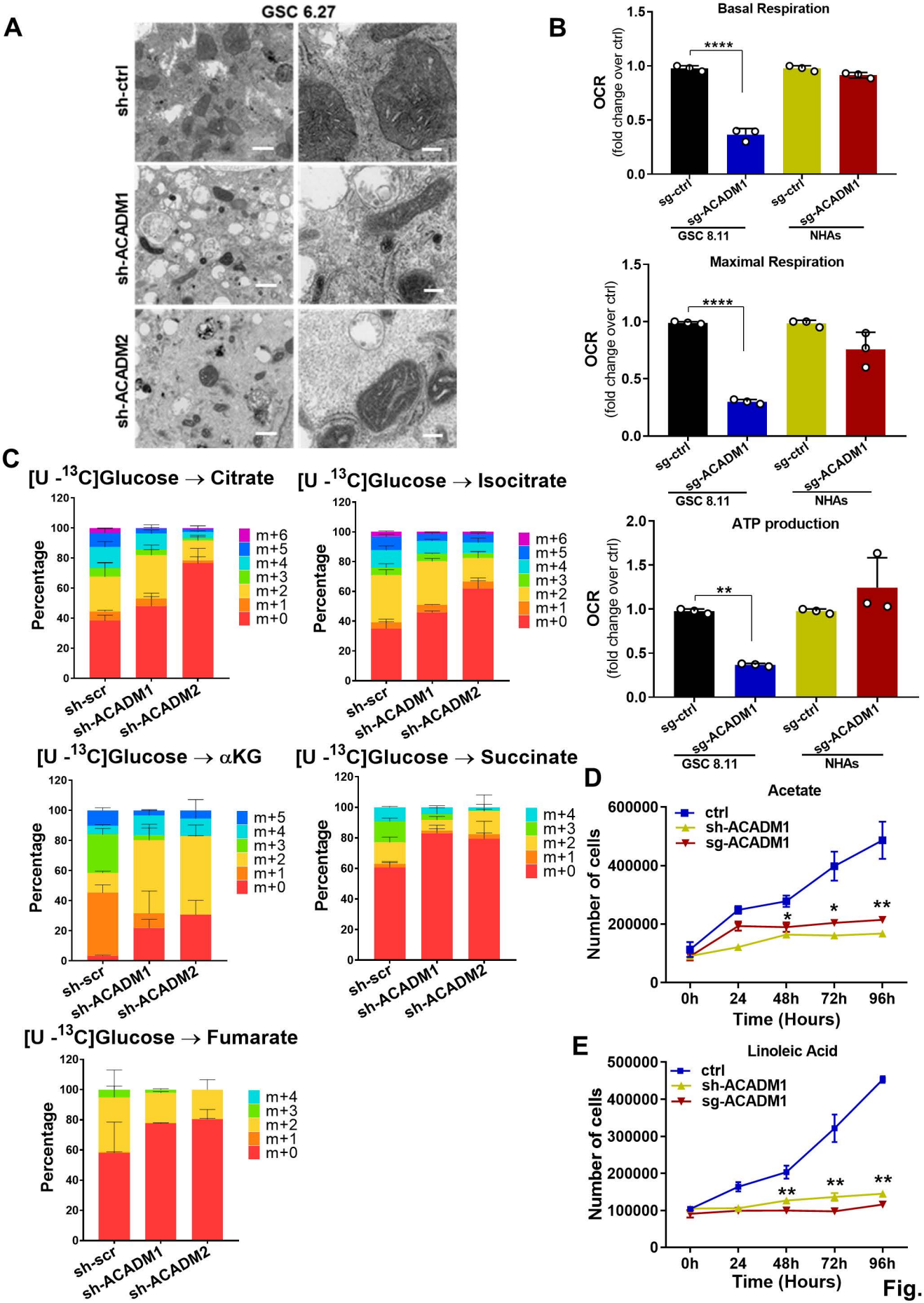
A
GSC 6.27
sh-ctrl
sh-ACADM1
sh-ACADM2
B
Basal Respiration
OCR
(fold change over ctrl)
****
sg-ctrl
sg-ACADM1
GSC 8.11
NHAs
Maximal Respiration
ATP production
**
C
[U -13C]Glucose → Citrate
[U -13C]Glucose → Isocitrate
[U -13C]Glucose → αKG
[U -13C]Glucose → Succinate
[U -13C]Glucose → Fumarate
Percentage
m+6
m+5
m+4
m+3
m+2
m+1
m+0
sh-scr
sh-ACADM1
sh-ACADM2
D
Acetate
Number of cells
ctrl
sh-ACADM1
sg-ACADM1
Time (Hours)
0h
24
48h
72h
96h
E
Linoleic Acid

Fig. S6

Figure S6. MCAD depletion alters the bioenergetics profile of GSCs.
a. Transmission electron microscopy images of mitochondria in GSC 6.27 upon MCAD silencing (magnification x15,000 and 50,000; scale bar= 1 µm, 300 nm). **b.** Analysis of basal respiration rate, maximal respiratory capacity, and ATP-linked respiration generated via metabolic flux assay. Rates are quantified by normalization of OCR level to the total protein OD values. *P* values were generated using Kruskal–Wallis ANOVA. Dunn's test for comparison among groups $^{**}P = 0.01$, $^{****}P = 0.0001$. Results represent cumulative analyses of multiple independent biological replicates from three independent experiments (n≥4 for each condition per experiment). Data extracted from the OCR traces in Figure 3C, D. **c.** Isotopologue patterns for incorporation of ^{13}C-labeled glucose into TCA cycle intermediates, as measured by LC-MS in GSC 8.11 infected with anti-*ACADM* or control shRNA. Cells were cultured with ^{13}C glucose for 24 hours prior to sample collection. N = 3 biological replicates, error bars = +/- SD. **d., e.** 96-h growth curve of GSC 8.11 cells upon *ACADM* silencing with shRNA/sgRNA cultured in DMEM-F12 media supplemented with acetate (2 mM) (d) or linoleic acid (0.1 mg/ml) (e). Day 0 was defined as 48 hours of puromycin selection. Values represent the mean ± SD of three independent experiments. *P* values were generated using Kruskal–Wallis ANOVA. Dunn's test for comparison among groups. In **d**: $^{*}P = 0.011$ $^{**}P = 0.003$. In **e**: $^{**}P \leq 0.0033$.

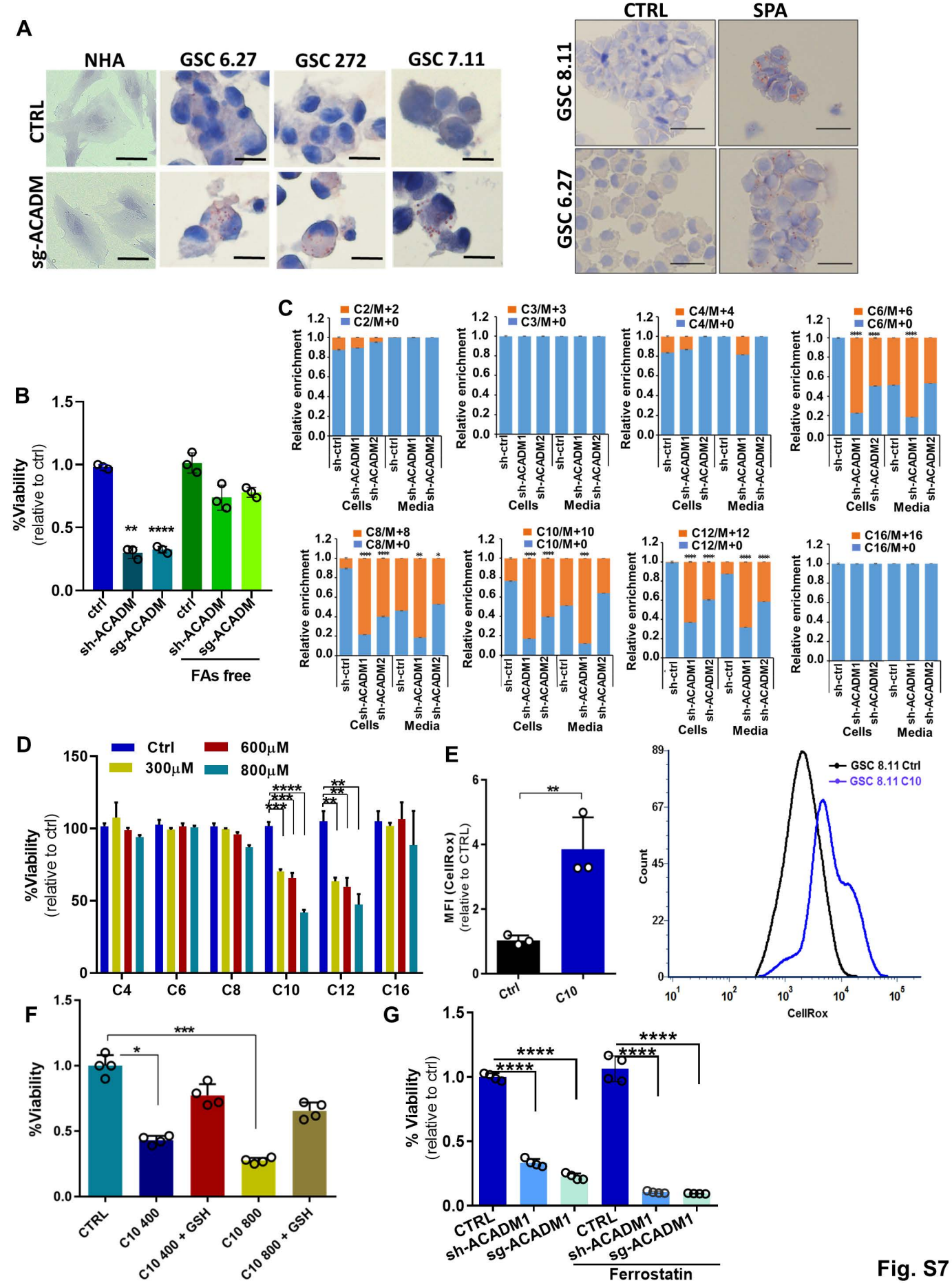
A
NHA
GSC 6.27
GSC 272
GSC 7.11
CTRL
sg-ACADM
CTRL
SPA
GSC 8.11
GSC 6.27
B
%Viability
(relative to ctrl)
ctrl
sh-ACADM
sg-ACADM
FAs free
C
C2/M+2
C2/M+0
C3/M+3
C3/M+0
C4/M+4
C4/M+0
C6/M+6
C6/M+0
C8/M+8
C8/M+0
C10/M+10
C10/M+0
C12/M+12
C12/M+0
C16/M+16
C16/M+0
Relative enrichment
sh-ctrl
sh-ACADM1
sh-ACADM2
Cells
Media
D
Ctrl
300μM
600μM
800μM
%Viability
(relative to ctrl)
C4
C6
C8
C10
C12
C16
E
MFI (CellRox)
(relative to CTRL)
Ctrl
C10
GSC 8.11 Ctrl
GSC 8.11 C10
Count
CellRox
F
%Viability
CTRL
C10 400
C10 400 + GSH
C10 800
C10 800 + GSH
G
% Viability
(relative to ctrl)
CTRL
sh-ACADM1
sg-ACADM1
Ferrostatin

Fig. S7

Figure S7. Toxic lipid species are causally correlated with ROS increase and cell death in MCAD-silenced GSCs. a. (Left) Oil Red O staining in NHAs, GSCs 6.27, 272, 7.11 cells infected with sgRNA targeting either *ACADM* or GFP at 72 hours from the silencing, Scale bar = 10 μm. (Right) Oil Red O staining of GSC 8.11 and 6.27 cells after 72-hour treatment with SPA. DMSO was used as control, scale bar 50 μm. **b.** Cell viability as assessed by Trypan Blue exclusion in *ACADM* wild type or null GSC 8.11 grown in normal or FAs-free DMEM-F12 7 days after puromycin selection. Data represent the mean ± SEM of three biologically independent replicates. *P* values were generated using Kruskal–Wallis ANOVA. Dunn's test for comparison among groups. ***P* < 0.01, **** *P* = 0.0001. **c.** LC-MS acyl-carnitine labeling profile of growth medium and whole-cell extracts from GSC 8.11 infected with anti-*ACADM* or non-targeting shRNAs cultured with ^{13}C oleate for 24 hours prior to sample collection. N = 3 biological replicates, error bars represent ± SD. *P* values were generated using Kruskal–Wallis ANOVA. Dunn's test for comparison among groups. **P* = 0.04, ** *P* = 0.0032 *** *P* = 0.0002, **** *P* <0.0001. **d.** Cell viability assessed by Trypan Blue exclusion of GSC 8.11 cells treated with 400 μM butyrate (C4), hexanoate (C6), octanoate (C8), decanoate (C10), dodecanoate (C12), palmitic acid (C16), or vehicle control for 48 h. Data represent mean ± SEM of four biologically independent replicates *P* values were generated using Kruskal–Wallis ANOVA. Dunn's test for comparison among groups. ***P* < 0.006; ****P* < 0.0003; *****P* <0.0001. **e.** Quantification by flow cytometry of ROS production in GSC 8.11 cells treated with C10 for 48 h measured by CellROX Green (left) and representative fluorescence (right). Data represent mean ± SEM of three biologically independent replicates. *P* values were generated using two-tailed t-test. ***P* = 0.0082. **f.** Viability of GSC 8.11 cells grown for 48 h in medium supplemented with 400 or 800 μM C10 and in the presence or absence of GSH- ethyl ester (GSH-EE) assessed by Trypan Blue exclusion. Data represent mean ± SEM of four biologically independent replicates. *P* values were generated using Kruskal–Wallis ANOVA. Dunn's test for comparison among groups. **P*= 0.0163; *** *P*= 0.0005. **g.** Quantification of cell viability as assessed by Annexin V in *ACADM*-wild type or -null GSCs 272 cells grown in DMEM supplemented with ferrostatin-1 (0.5 μM) 7 days after puromycin selection. Data represent the mean ± SEM of four biologically independent replicates. *P* values were generated using Kruskal–Wallis ANOVA. Dunn's test for comparison among groups. **** *P* <0.0001.

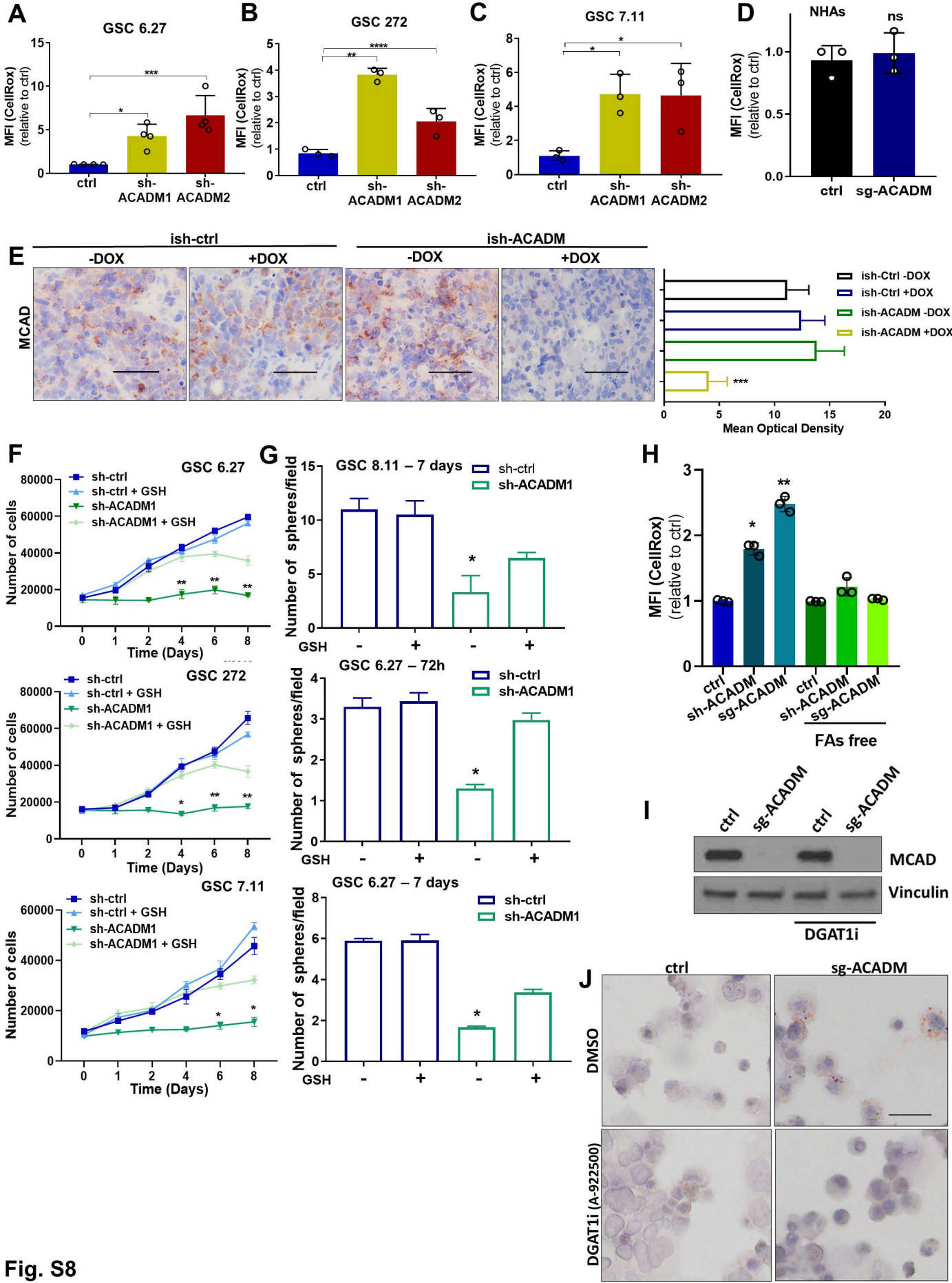
A
GSC 6.27
MFI (CellRox) (relative to ctrl)
ctrl
sh-ACADM1
sh-ACADM2
B
GSC 272
C
GSC 7.11
D
NHAs
ns
ctrl
sg-ACADM
E
ish-ctrl
ish-ACADM
-DOX
+DOX
MCAD
ish-Ctrl -DOX
ish-Ctrl +DOX
ish-ACADM -DOX
ish-ACADM +DOX
Mean Optical Density
F
GSC 6.27
GSC 272
GSC 7.11
sh-ctrl
sh-ctrl + GSH
sh-ACADM1
sh-ACADM1 + GSH
Number of cells
Time (Days)
G
GSC 8.11 – 7 days
GSC 6.27 – 72h
GSC 6.27 – 7 days
Number of spheres/field
GSH
H
MFI (CellRox) (relative to ctrl)
ctrl
sh-ACADM
sg-ACADM
FAs free
I
MCAD
Vinculin
DGAT1i
J
ctrl
sg-ACADM
DMSO
DGAT1i (A-922500)

Fig. S8

Figure S8. MCAD knockdown triggers ROS-related damage in GSCs *in vitro* and *in vivo*. a,b,c. Quantification of ROS production (mean of fluorescence intensity) as measured by CellROX Green in GSC 6.27 **(a)**, 272 **(b)** and 7.11 **(c)** cells harboring anti-*ACADM* or non-targeting shRNA. Values represent the mean ± SD of three or four independent experiments. *P* values were generated using Kruskal–Wallis ANOVA. Dunn's test for comparison among groups. **(a)** **P* = 0.025, ****P* = 0.0009, **(b)** ***P* = 0.007, *****P* < 0.0001, **(c)** **P* < 0.03. **d.** Quantification of ROS production (mean of fluorescence intensity) as measured by CellROX Green in NHAs harboring anti-*ACADM* sgRNA at 72 hours from the silencing. **e.** Immunostaining for MCAD of xenograft tumor samples derived from GSC 8.11 harboring doxycycline-inducible anti- *ACADM* or non-targeting shRNAs (shown in Figure S5D) and relative quantification. Quantification was performed with ImageJ software, four/five images per condition, where each condition was represented by three biological replicates. Values are expressed as mean ± SD; *P* values were generated using Kruskal– Wallis ANOVA. Dunn's test for comparison among groups. *** *P* = 0.0002. **f.** Growth curves of GSC 6.27, 272 and 7.11 cells infected with sh-*ACADM* or non-targeting shRNAs grown in the presence or absence of GSH-EE. Values are expressed as mean ± SD; *P* values were generated using Kruskal–Wallis ANOVA. Dunn's test for comparison among groups. GSC 6.27, ** *P*< 0.007; GSC 272 **P* = 0.03, ** *P* ≤ 0.004; GSC 7.11 **P* ≤ 0.04. **g.** Quantification of the number of spheres formed by GSC 8.11 and GSC 6.27 harboring sh-*ACADM* or non-targeting shRNAs grown for 7 days (for 8.11) or 72 hours and 7 days (for 6.27) in the presence or absence of GSH-EE as indicated. Values represent the number of spheres per field expressed as mean ± SD. *P* values were generated using Kruskal–Wallis ANOVA. Dunn's test for comparison among groups. **P* ≤ 0.04. **h.** Quantification of ROS via CellRox Green staining intensity by flow cytometry in *ACADM* wild type or null GSC 8.11 cells grown in normal or FAs free DME-F12 supplemented. Mean values ± SD of three biologically independent replicates. *P* values were generated using Kruskal–Wallis ANOVA. Dunn's test for comparison among groups. **P* < 0.05, ***P* = 0.01. MFI= Mean of Fluorescence Intensity. **i.** Representative immunoblot of MCAD expression in GSC 8.11 infected with *ACADM*-targeting or control sgRNA in the presence or in the absence of DGAT1 inhibitor. Vinculin served as a loading control. **j.** Oil Red O staining of GSC 8.11 cells upon MCAD ablation in the presence or in the absence of DGAT1 inhibitor (A-922500, 15μM). DMSO was used in the control. Scale bar= 50 μm.